Acta Odontologica Scandinavica, 2012; 70: 603–609

informa
healthcare

ORIGINAL ARTICLE

Back-scattered and secondary electron images of scanning electron microscopy in dentistry: a new method for surface analysis

MOHAMMAD ALI SAGHIRI[1], KAMAL ASGAR[2], MEHRDAD LOTFI[3], KASRA KARAMIFAR[4], ALI MOHAMMAD SAGHIRI[5], PRASANNA NEELAKANTAN[6], JAMES L. GUTMANN[7] & AHMAD SHEIBANINIA[8]

[1]*Department of Dental Material, Dental Branch, Islamic Azad University, Tehran, Iran,* [2]*Department of Dental and Biological Materials, University of Michigan, Michigan, USA,* [3]*Research Center for Pharmaceutical Nanotechnology and Department of Endodontics, Dental Faculty, Tabriz University (Medical Sciences), Tabriz, Iran,* [4]*Department of Endodontics, Dental Branch, Islamic Azad University, Tehran, Iran,* [5]*Department of Computer Engineering, Amirkabir University of Technology, Tehran, Iran,* [6]*Department of Conservative Dentistry and Endodontics, Saveetha Dental College, Saveetha University, Chennai, India,* [7]*Baylor College of Dentistry, Texas A&M Health Science Center, Dallas, Texas, USA, and* [8]*Department of orthodontic, Dental Branch, Islamic Azad University, Tehran, Iran*

Abstract

Objective. A scanning electron microscope (SEM) is a popular tool for investigating the root canal surface to visualize dentinal tubules, the smear layer and various root canal filling materials in endodontics. Most of the SEM micrographs taken in endodontic research are in secondary electrons (SE) mode, in which the topographic view of a subject can be demonstrated without giving any information about the real structure. Back-scattered electron (BSE) images are also used, which reveal some information about the internal structure while providing no topographic details. The aim of this study was to investigate the possibility of using back-scattered (BSE) and secondary electron (SE) mode of scanning electron microscopy (SEM) together for obtaining detailed information about biomaterials in relation to dental structures. ***Materials and methods.*** Mesiobuccal roots of four permanent maxillary molars were cleaned and shaped with rotary instruments. Two samples were obturated with gutta-percha and sealer. After 2 weeks, gutta-perch was removed using rotary instruments and chloroform. In the other phase of the study, white mineral trioxide aggregate was mixed and packed into five glass tubes and exposed to blood, deionized water, synthetic tissue fluid and egg white. All the samples were prepared for visualization under SE and BSE modes of SEM to observe the characteristics of material remnants and surface structures. ***Results.*** BSE mode illustrated different grey scale views which made it possible to differentiate dentin chips from filling material remnants on the surface of root canal dentin. In addition, SE mode focused on image topography, while a BSE detector showed new texture formation on the surface of white mineral trioxide aggregate exposed to proteinaceous fluids such as blood or egg white. ***Conclusions.*** Mapping BSE and SE micrographs helped us to better understand the structure of materials on the surface of root canal dentin and MTA. Moreover, analysis of structure of materials on the surface of root canal dentine and MTA can be performed better by mapping of BSE and SE micrographs.

Key Words: *back-scattered, endodontics, secondary electron, scanning electron microscopy*

Introduction

A scanning electron microscope (SEM) is a powerful tool for microstructural evaluation of dental materials [1-3]. In this technique, an electron beam scans the surface of the sample to produce a variety of signals, the characteristics of which depend on many factors, including the energy of an electron beam and the nature of the sample.

Three types of signals provide the greatest amount of information in SEM: the secondary electrons (SE), back-scattered electrons (BSE) and x-rays [4]. A schematic diagram of these signals is shown in Figure 1. SE are emitted from the atoms on the surface, which produce a readily interpreted image, the contrast of which is determined by the sample morphology. The small diameter of the primary electron beam helps in obtaining a high resolution image.

Correspondence: Mohammad Ali Saghiri, Assistant Professor, Department of Dental Material, Dental Branch, Islamic Azad University, Tehran Branch, PO Box 14665-1445, Tehran, Iran. E-mail: saghiri@gmail.com

(Received 25 December 2010; revised 8 June 2011; accepted 14 September 2011)

ISSN 0001-6357 print/ISSN 1502-3850 online
DOI: 10.3109/00016357.2011.645057

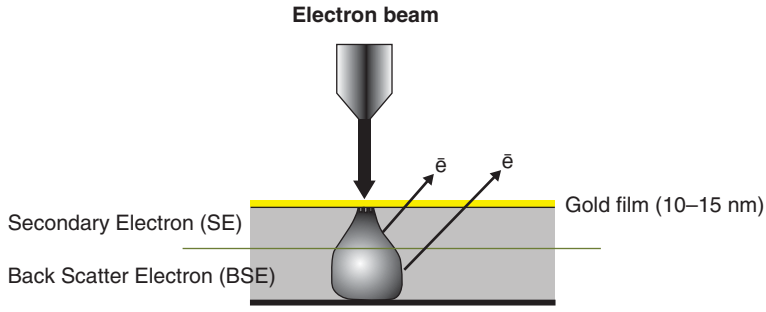

Figure 1. Schematic diagram of SEM principles and electron interaction.

Back-scattered electrons are primary beam electrons that are reflected from atoms. The atomic number of the sample elements determines the image contrast of a back-scattered micrograph [5]. Therefore, the image obtained by back-scattered mode will show the distribution of different chemical phases in a sample. However, the resolution in such an image is not as good as that obtained through the secondary electrons due to emission of electrons from different depths in the sample [6].

Root canal instrumentation produces a smear layer on the surface of the prepared root canal walls. This layer contains both inorganic and organic substances [7]. Only a handful of studies have been performed to make a distinction between dentin chips, the smear layer and root filling material remnants using SEM micrographs of the root canal. SEM micrographs have been used for evaluating the surface characteristics including roughness, porosity and uniformity [8]. It has not been used for detecting surface crystallography and making distinctions between particles on a surface. With knowledge about the endodontic biomaterial interfaces such as mineral trioxide aggregate (MTA) and root canal walls, clinicians will be able to better predict the interaction behavior of endodontic biomaterials.

As there are indeed several manuscripts in the literature that have been published using one or both of these modalities of SEM [1-4,8,9], this study qualitatively evaluated changes in some endodontic biomaterials' constituent phases on SEM micrographs by mapping secondary and back-scattered micrographs concomitantly with special emphasis on factors that are mostly relevant to the surface analysis for observation by SEM, including the type of detectors and their applications.

Materials and methods

Part 1: SEM of root canal dentin and observation of material remnants

Human maxillary first permanent molars (n = 4) extracted for periodontal reasons with mesiobuccal canal curvatures ranging between 30–35° and similar root lengths were selected. After access cavity preparation, the working lengths were determined using a K-file #10 (Dentsply Maillefer, Ballaigues, Switzerland) and confirmed by radiographs. The mesiobuccal canals were instrumented using RaCe rotary files (FKG Dentaire, La Chaux-de Fonds, Switzerland) up to an apical size of 30.06. One milliliter of 5.25% NaOCl was used as an irrigant between each instrument using a 28-gauge needle (Dentsply Tulsa Dental, Tulsa, OK); following instrumentation, canals were flushed with 17% EDTA for 1 min and subsequently dried with paper points. Two specimens were obturated with gutta-percha (Meta Dental Co, Korea) and AH 26 sealer (De Trey-Dentsply, Konstanz, Germany) by lateral compaction technique, while the other two specimens were left unobturated and served as controls. Radiographs were taken in buccolingual and mesiodistal directions to confirm the adequacy of obturation. After placing a temporary restoration (Zonalin, Masterdent, New York, NY), each tooth was stored in a humidor at 37°C for 2 weeks. Following removal of the temporary filling, coronal 5 mm of the root filling material was removed using Gates-Glidden drills #2 and #3 (Maillefer, Ballaigues, Switzerland). RaCe rotary files (FKG Dentaire, La-Chaux-de-Fonds, Switzerland) were used along with chloroform (0.2 mL) to remove the remaining material. The working length was regained gradually and the canals were further instrumented up to apical size of 40.04. The root canals were irrigated with 5.25% NaOCl during instrumentation. The process of retreatment was considered complete when there was no evidence of filling materials on the files. The canals were irrigated with 17% EDTA, flushed with distilled water and dried with paper points. All the procedures were performed by a same operator.

The roots were grooved vertically with diamond discs (Brasseler, Savannah, GA) on the buccal and lingual surfaces. All four specimens were split into two halves longitudinally using a chisel and mallet. Half of each sample was chosen, placed in 2% glutaraldehyde for 24 h and then rinsed 3-times with a sodium cacodylate buffered solution (0.1 M, pH 7.2). After incubation in osmium tetroxide for 1 h, the samples were dessicated with ascending concentrations of

ethyl alcohol (30–100%), placed in a dessicator for 24 h and mounted on a metallic stub and observed under SEM for obturating material remnants and debris at the coronal, middle and apical portions of the canal.

Part 2: Analysis of white mineral trioxide aggregate (WMTA) exposed to different biological fluids

Two sachets of White MTA (ProRoot MTA, Dentsply-Tulsa, OK) were mixed separately with distilled water under aseptic conditions according to manufacturer's instructions. MTA was packed into five cylindrical polycarbonate tubes with an 8 mm inner diameter and 10 mm height. All the specimens were prepared for exposure to various biological fluids and placed in separate vials and stored at 37°C and 100% relative humidity for 24 h to ensure complete setting of WMTA. After 24 h, wet pieces of gauze soaked in blood, deionized water, synthetic tissue fluid and egg white were placed on each specimen ($n = 4$) for 24 h. Wet gauze pieces were replaced every 6 h with fresh ones. The fifth specimen served as control.

SEM analysis

The root canal samples and WMTA specimens were placed in a dessicator for 24 h and mounted on a metallic stub. After sputter-coating with gold, SEM micrographs were taken (Leo 440i (Oxford, UK) equipped with a back-scatter detector (Oxford Instruments, Abingdon, UK) and visualized under both BSE and SE detectors). Several micrographs were taken in each mode at various zones of each specimen at two different magnifications (2500 × and 5000 × for part 1; 1000 × for part 2), at 15 kV and 1 nA of probe current. There were two reasons for selecting these magnifications: These magnifications have been used for detecting dentinal tubules and smear layer. In essence, an image at these magnifications would show dentinal tubules, smear layer and remaining gutta-percha and dentinal chips, enhancing the ability to compare the different materials. At higher magnifications, only one of these components may appear per image, which would not help in comparative identification. In analyzing MTA exposed to different biological fluids, 1000 × magnification was employed in order to observe an heterogeneous structure of MTA crystals over a large field and to obtain a correct average composition after exposure to some different biological fluids.

Results

SEM micrographs of root canal dentin (Figure 2) showed two distinguishable phases on the dentinal surfaces in the apical, middle and coronal thirds. Foreign particles can be seen on the surface of root canal dentin with different shades. In addition, some particles are not significantly different in contrast to both SE and BSE. No significant differences were observed in the SEM micrographs of both SE and BSE modes in unobturated samples.

In WMTA specimens SE and BSE mapping of samples exposed to blood, synthetic tissue fluid and egg white showed a complex texture of mineral phases with highly visible covered surfaces of the MTA specimens, especially in proteinaceous fluid groups such as blood and egg white. There was no notable difference in micrograph brightness between SE and BSE of WMTA exposed to deionized water and blank specimen (Figure 3). The effectiveness of BSE contrast images can be seen in Figures 2 and 3 (right column).

Discussion

This study analyzed the usefulness of two imaging modes of SEM in studying two different aspects of endodontic treatment—re-treatment and interactions between endodontic biomaterials and tooth structure. Success of root canal re-treatment depends on complete eradication of micro-organisms and removal of the previous filling materials. Although it still remains questionable whether this outcome variable (filling remnants in the root canal) is directly related to clinical outcomes, complete removal of old filling material from the root canal system is mandatory to achieve adequate debridement of the area and a fluid impervious seal following obturation and re-establish periapical tissue health [10].

In order to determine the canal cleanliness after different methods of root-filling removal, several *in vitro* methods have been used. This kind of microstructural evaluation is necessary in order to identify the most efficient means of complete removal of root-filling. Stereomicroscopy has been commonly used to detect the remnants of root-filling material following re-instrumentation, but this method gives only a macroscopic view. It is not possible to observe presence of materials at the microscopic level and its distribution in relation to dentineal tubules with this technique [9,11].

Another parameter of importance in root canal treatment is the interaction of endodontic biomaterials with the root canal walls in the presence of biological fluids. One of the most commonly used materials in endodontics is MTA. The mineralization characteristics and biocompatibility of MTA are influenced by the presence of biological fluids. In general, formation of hydroxyapatite precipitates on the surface of MTA influences the biocompatibility of this material [12]. Addition of proteinaceous fluids (e.g. blood, enriched albumin solution–egg white) ameliorates the toxicity of WMTA by apatite formation, while synthetic tissue fluid is a protein-free solution containing high ionic saturations [13,14].

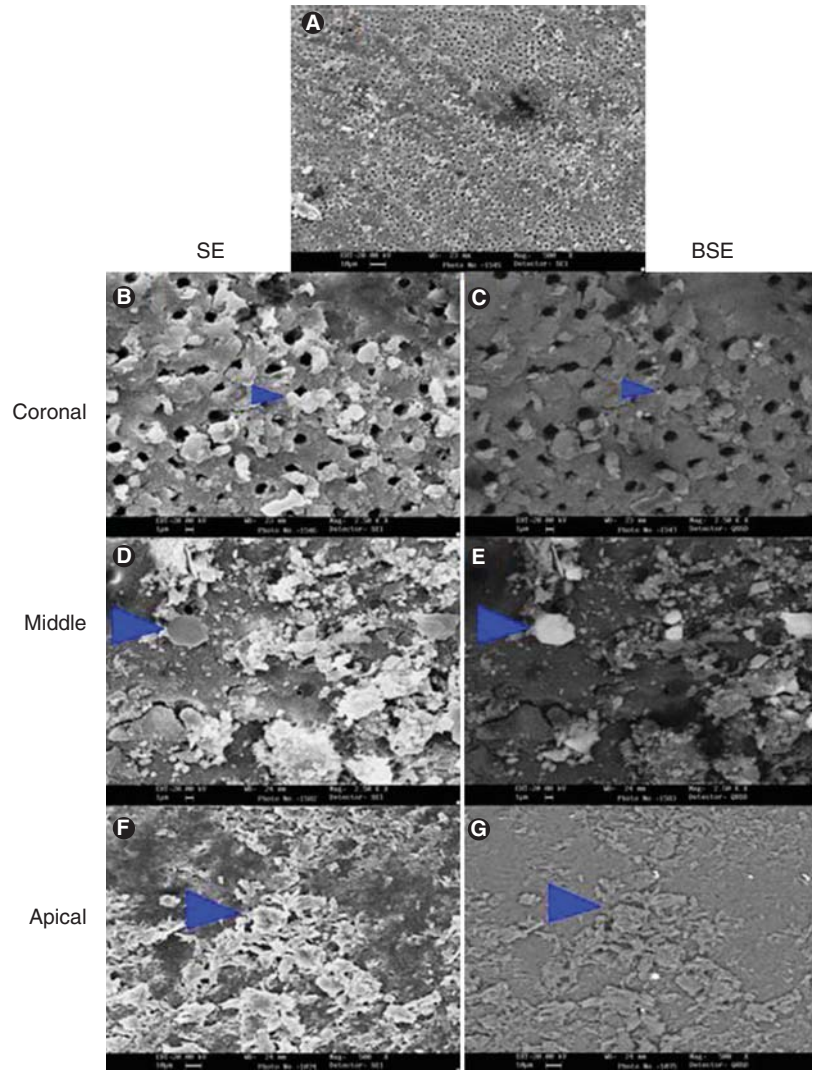

Figure 2. Mapping SE and BSE of root canal dentin is illustrated in (B, C), (D, E) and (F, G) in the coronal, middle and apical portions, indicating some gutta-percha remnants and dentin chips. Lighter-contrast particles indicate compositional contrast, further confirming that they are gutta-percha and (A) overview of root canal wall.

Recent developments in SEM help in obtaining various types of images through different modes (SE, BSE, Auger and Cathodoluminescence) from the specimen without altering the specimen or beam geometry [15,16]. This technique is qualitative. The contrast changes across particles due to discrimination of atomic number, with some particles have different shades in SE and BSE micrographs [17]. Both BSE and SE micrographs have several advantages. It would be unwise to preferentially recommend one technique over the other [18]; however, the advances in BSE technology and applications have made its use increasingly popular in studying the microstructure of dental materials. BSE micrographs have been used for analysis of grain boundary distributions [19], phase identification [20,21] and plastic strain analysis [22].

Acceleration voltage (increasing the energy of an electron beam) allows electrons to penetrate deeper into the specimens. The higher the acceleration voltage, the deeper is the penetration of electrons into the sample [23]. As a result, ultrastructural information from deeper layers will interfere with that from the surface morphology. If acceleration voltage is lowered, a better quality of the endodontic biomaterials surface morphology and structures can be seen. However, using high acceleration voltage will destroy the specimens due to increased specimen temperature [24]. During SEM analysis, electrons interact with the surface and raise the surface temperature, causing evaporation or sublimation of oily or organic substances, which may thus become undetectable.

Decreasing the accelerating voltage (kV) may prevent this event at low magnifications. However, in dental material sciences, this is an area that is not well-documented. As a result, an acceleration voltage of 20 kV was used in the present study.

BSE micrographs have advantages over SE images in terms of showing the compositional contrast. This

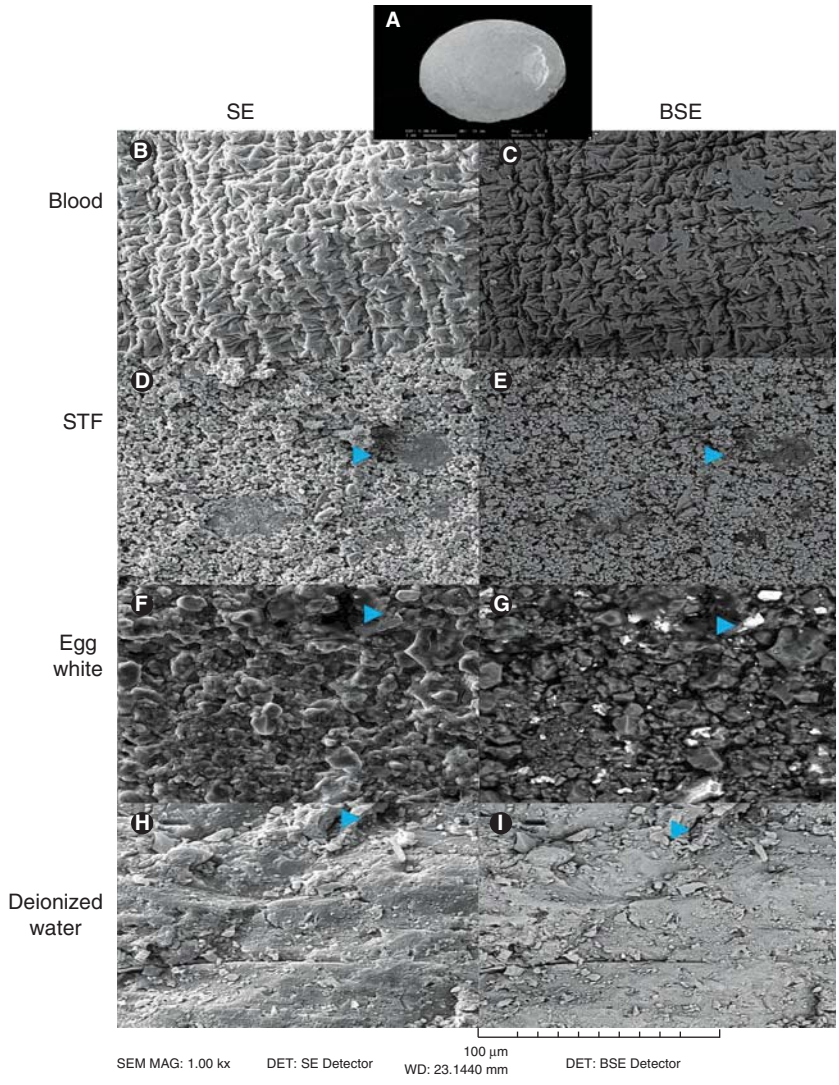

Figure 3. Mapping SE and BSE of WMTA tablets is demonstrated in (B, C), (D, E), (F, G) and (H, I) in blood, synthetic tissue fluid, egg white and deionized water, respectively. Gleaming spots can be easily detected in the synthetic tissue fluid group and prominent bright blanket (the brighter surface of MTA exposed to blood as detected in BSE micrographs, as compared to SE images, indicating that the sample was covered by new molecules of a new texture and higher atomic number than it was prior to exposure to blood) are detected in blood, but no differences between micrographs of deionized water and blank specimens can be seen and (A) overview of WMTA tablet.

parameter helps in distinguishing the distribution of elements on the surface being analyzed. Higher-atomic elements appear brighter in BSE [24-26]; therefore, differences in the grey levels observed in root canal walls allow distinction between gutta-percha and dentine chips in descending order of brightness. Similar to the hardened cement paste exposed to blood, a brighter texture can be observed, which is indicative of a higher-atomic polycrystalline structure such as carbonated hydroxyapatite, unlike ingredients of WMTA such as calcite or calcium silicate oxide covering WMTA tablets after exposure to blood.

In general, cell observation under SEM requires prior use of a fixative like osmium tetroxide and glutaraldehyde. This process of fixation is usually performed by incubation in a solution of a buffered chemical fixative, such as glutaraldehyde, sometimes in combination with formaldehyde and other fixatives and optionally followed by post-fixation with osmium tetroxide. Nevertheless, it was not within the scope of this present paper to observe the cell adhesion to surface and other biological interactions in detail, on the surface of WMTA. The aim was only limited to observing the effect of different biological fluids on the surface characteristics of MTA. For this reason, samples were not fixed prior to examination. However, a fixative was employed in part 1 of this study to analyze the smear layer along with dentinal chips, as suggested by Torabinejad et al. [27] and Carvalho et al. [28].

When both techniques were used together at the same point and the same time (mapping of both images and comparison), we would end up identifying

several new features or clear several misinterpreted features that have been identified as a result of using one of the methods alone, which some studies in the past have done. However, they have used only one of the imaging modalities, and hence the results may have been wrongly interpreted. Therefore, this study is of paramount value in contemporary endodontic research. The application of the two imaging modalities in isolation may not yield correct facts and, in fact, it may be possible that conclusions in the past based on just one of these methods are erroneous. Therefore, the need to use both of these features at the same time to examine each area is important to reach correct results in imaging studies.

The type of sputtering used in this study merits discussion. For conventional imaging in the Scanning Electron Microscope (SEM), specimens must be electrically conductive, at least at the surface, and electrically grounded to prevent the accumulation of electrostatic charge at the surface. Metal objects require little special preparation for SEM except for cleaning and mounting on a specimen stub. Non-conductive specimens tend to charge when scanned by the electron beam, and especially in secondary electron imaging mode, this causes scanning faults and other image artifacts [5]. They are therefore usually coated with an ultra-thin coating of electrically-conducting material, commonly gold, deposited on the sample either by low vacuum sputter coating or by high vacuum evaporation. Conductive materials in current use for specimen coating include gold, gold/palladium alloy, platinum, osmium, iridium, tungsten, chromium and graphite [15]. Coating prevents the accumulation of static electric charge on the specimen during electron irradiation. There are two reasons for coating, even when there is enough specimen conductivity to prevent charging: (i) to increase signal and surface resolution, especially with samples of low atomic number (Z); and (ii) improvement in resolution arises because backscattering and secondary electron emission near the surface are enhanced and thus an image of the surface is formed. In the present study we used gold instead of other sputtering material such as carbon, since gold has a high atomic number and sputter coating with gold produces high topographic contrast and resolution. However, the coating has a thickness of a few nanometers and can obscure the underlying fine detail of the specimen at very high magnification. In addition, a previous study showed the practical suitability of using gold for checking the surface topography of Mineral Trioxide aggregate (MTA) [29,30]

In the current study, SE and BSE were used concomitantly to observe deep layers of root canal walls. WMTA and root canal wall were selected as examples relevant to research in endodontics, but it can become a principle for studying other dental/medical materials. From the current study, it was possible to infer that there was no notable difference in micrograph brightness between SE and BSE images which are marked by ▶ (Figures 2 and 3). Furthermore, as evidenced in Figures 3B and C, brightness changed in all parts of the image uniformly. This may be, in part, due to the effect of some chemical changes on the surface. This may be attributed to the exchange of some element on the surface of WMTA due to exposure to blood.

It can be concluded that mapping BSE and SE micrographs are useful in differentiating materials and remnants on the surface of root canals. Also, these methods are also useful in analyzing the surface of biomaterials accurately and, hence, can be recommended as useful tools in endodontic research.

Declaration of interest: The authors report no conflicts of interest. The authors alone are responsible for the content and writing of the paper.

References

[1] McComb D, Smith DC. A preliminary scanning electron microscopic study of root canals after endodontic procedures. J Endod 1975;1:238–42.

[2] Yamada RS, Armas A, Goldman M, Lin PS. A scanning electron microscopic comparison of a high volume final flush with several irrigating solutions: part 3. J Endod 1983; 9:137–42.

[3] Saleh IM, Ruyter IE, Haapasalo MP, Orstavik D. Adhesion of endodontic sealers: scanning electron microscopy and energy dispersive spectroscopy. J Endod 2003;29:595–601.

[4] Kato M, Homma K, Komura F, Furuya T. Scanning electron microscope. United States patents US Patent 4,803,358. 1989.

[5] Lloyd GE. Atomic number and crystallographic contrast images with the SEM: a review of backscattered electron techniques. Mineral Mag 1987;51:3–19.

[6] Cole DA, Shallenberger JR, Novak SW, Moore RL. SiO2 thickness determination by x-ray photoelectron spectroscopy, Auger electron spectroscopy, secondary ion mass spectrometry, Rutherford backscattering, transmission electron microscopy, and ellipsometry. J Vac Sci Technol B 2000; 18:440–4.

[7] Torabinejad M, Handysides R, Khademi AA, Bakland LK. Clinical implications of the smear layer in endodontics: a review. Oral Surg Oral Med Oral Pathol Oral Radiol Endod 2002;94:658–66.

[8] Garberoglio R, Brännström M. Scanning electron microscopic investigation of human dentinal tubules. Arch Oral Biol 1976;21:355–62.

[9] Mannocci F, Innocenti M, Ferrari M. Stereomicroscopic and scanning electron microscopic study of roots obturated with vertically condensed gutta-percha, epoxy resin cement, and dentin bonding agent. J Endod 1998;24:397–400.

[10] Bergenholtz G, Lekholm U, Milthon R, Heden G, Odesjö B, Engström B. Retreatment of endodontic fillings. Scand J Dent Res 1979;87:217–24.

[11] Somma F, Cammarota G, Plotino G, Grande NM, Pameijer CH. The effectiveness of manual and mechanical instrumentation for the retreatment of three different root canal filling materials. J Endod 2008;34:466–9.

[12] Yasuda Y, Ogawa M, Arakawa T, Kadowaki T, Saito T. The effect of mineral trioxide aggregate on the mineralization

ability of rat dental pulp cells: an *in vitro* study. J Endod 2008; 34:1057–60.

[13] Danesh F, Tootian Z, Jahanbani J, Rabiee M, Fazelipour S, Taghva O, et al. Biocompatibility and mineralization activity of fresh or set white mineral trioxide aggregate, biomimetic carbonated apatite, and synthetic hydroxyapatite. J Endod 2010;36:1036–41.

[14] Saghiri MA, Asgar K, Daliri M, Lotfi M, Delvarani A, et al. Morphological behavior and attachment of p19 neural cells to root-end filling materials. Scanning 2010;32:369–74.

[15] Olsen SL. Introduction: applications of scanning electron microscopy to archaeology. In: British Archaeological Society Scanning electron microscopy in archaeology. Oxford: British Archaeological Reports; 1988. p 3–7.

[16] Prior DJ, Boyle AP, Brenker F, Cheadle MC, Day A, Lopez G, et al. The application of electron backscatter diffraction and orientation contrast imaging in the SEM to textural problems in rocks. Am Mineral 1999;84:1741–59.

[17] Reed SJB. Electron microprobe analysis and scanning electron microscopy in geology. 2nd ed. Cambridge: Cambridge University Press; 2005. p 55–61.

[18] Dingley D. Progressive steps in the development of electron backscatter diffraction and orientation imaging microscopy. J Microsc 2004;213:214–24.

[19] Dingley DJ, Randle V. Microtexture determination by electron back-scatter diffraction. J Mater Sci 1992;27: 4545-66.

[20] Baba-Kishi KZ, Dingley DJ. Backscatter Kikuchi diffraction in the SEM for identification of crystallographic point groups. Scanning 1989;11:305–12.

[21] Michael JR, Goehner RP. Crystallographic phase identification in the scanning electron microscope: backscattered electron kikuchi patterns imaged with a CCD-Based detector. MSA Bulletin 1993;23:168.

[22] Kamaya M, Wilkinson AJ, Titchmarsh JM. Quantification of plastic strain of stainless steel and nickel alloy by electron backscatter diffraction. Acta Mater 2006;54:539–48.

[23] Walther P, Autrata R, Chen Y, Pawley JB. Backscattered electron imaging for high resolution surface scanning electron microscopy with a new type YAG-detector. Scanning Microsc 1991;5:301–9; discussion 310.

[24] Pawley JB, Erlandsen SL. The case for low voltage high resolution scanning electron microscopy of biological samples. Scanning Microsc Suppl 1989;3:163–78.

[25] Frankel RS, Aitken DW. Energy-dispersive x-ray emission spectroscopy. Appl Spectrosc 1970;24:557–614.

[26] Bozzola JJ, Russell LD. Principles and techniques for biologists. In: Jones & Bartlett Publisher Electron microscopy. Sudbury: MA: John and Bartlett; 1999. p 50–71.

[27] Torabinejad M, Khademi AA, Babagoli J, Cho Y, Johnson WB, Bozhilov K, et al. A new solution for the removal of the smear layer. J Endod 2003;29:170–5.

[28] Carvalho AS, Camargo CH, Valera MC, Camargo SE, Mancini MN. Smear layer removal by auxiliary chemical substances in biomechanical preparation: a scanning electron microscope study. J Endod 2008;34:1396–400.

[29] Saghiri MA, Lotfi M, Joupari MD, Aeinehchi M, Saghiri AM. Effects of storage temperature on surface hardness, microstructure, and phase formation of white mineral trioxide aggregate. J Endod 2010;36:1414–18.

[30] Saghiri MA, Lotfi M, Saghiri AM, Vosoughhosseini S, Aeinehchi M, Ranjkesh B. Scanning electron micrograph and surface hardness of mineral trioxide aggregate in the presence of alkaline pH. J Endod 2009;35:706–10.